Spin-label EPR Approaches to Protein Interactions

Son, M. van

4

SPIN-SPIN INTERACTION IN RIGID 3_{10}-HELICAL PEPTIDES WITH TOAC SPIN LABELS: AN EPR POWER-SATURATION STUDY

4.1 Introduction

Electron paramagnetic resonance has become a powerful technique in biological structure determination. Most commonly, structure determination relies on measuring distances between paramagnetic centres, often spin labels, attached to specific positions in the biomacromolecules of interest. The most powerful techniques to measure such distances by EPR are limited in two aspects: they work for frozen solutions at low temperatures[1;2] and distance ranges between 0.8 – 1.5 nm are difficult to address[3]. Physiological conditions, such as liquid solutions at room temperature, pose additional challenges. The dipolar interaction between spins, so far the most reliable indicator for distance, can be partially averaged in liquid solution, and the isotropic exchange interaction J is a short-range interaction (several tenths of nanometres) and is difficult to interpret in terms of distance between spins. Also, in liquid solution, the spin-spin interaction is extracted from lineshape. Particularly, the difference in the spectra of the system of interest in the absence and the presence of the spin-spin interaction is evaluated, and therefore small spin-spin interactions and longer distances are difficult to measure. Here we show that for nitroxides, in the distance regime of 0.8 – 1.5 nm electron

spin-spin relaxation could be used as an indicator for distance, expanding the tools available to EPR so far even further towards biologically relevant conditions.

In this study, we determine the relaxation parameters by power-saturation experiments. We investigate a series of four rigid bi-radical peptides and corresponding size-matched mono-radical peptides described before[4]. The peptides consist of the non-coded, host α-amino acid α-aminoisobutyric acid (Aib), combined with one or two 4-amino-1-oxyl-2,2,6,6-tetramethyl-piperidine-4-carboxylic acid (TOAC) guest residues. The series consists of the bi-radicals $HEPTA_{3,6}$, $HEXA_{1,5}$, $OCTA_{2,7}$, $NONA_{2,8}$, and the mono-radicals $HEPTA_{6}$, $OCTA_{7}$, $NONA_{2}$, where the subscript indicates the TOAC positions. Exact sequences are given in Table 1 in reference [4]. In the previous study, the peptides where classified according to the magnitude of the exchange interaction: $HEPTA_{3,6}$ and $HEXA_{1,5}$ with a large exchange interaction and five-line EPR spectra as class I and $OCTA_{2,7}$ and $NONA_{2,8}$, with a small exchange interaction and three-line EPR spectra, as class II[4].

We demonstrate that in all cases the relaxation parameters of the bi-radicals differ significantly from the mono-radicals, showing that an additional relaxation mechanism operates in the bi-radicals. We attribute the additional relaxation to the spin-spin interaction in the bi-radicals and posit that it could be used as a tool for distance determination.

4.2 Material and methods

The synthesis of the peptides has been described previously, for $NONA_9$ and $NONA_{2,8}$ in reference [5], for $HEPTA_{3,6}$ in reference [6], for $HEPTA_6$, $HEXA_{1,5}$, $OCTA_{2,7}$, and $OCTA_7$ in reference [4]. The details about the sample preparation of the peptides are given in reference [4].

EPR measurements

The series of microwave-power saturation experiments were done at 9.7 GHz using an ELEXSYS E 680 spectrometer (Bruker BioSpin GmbH, Rheinstetten, Germany) equipped with a dielectric cavity. The peptides were measured over a range of 0.2 W to 0.2 mW of microwave power, in steps of 1dB attenuation. The measurements were done with a field sweep of 15 mT, 2048 field points, a time constant of 5.12 ms, and a conversion time of 5.12 ms. The modulation frequency was 100 kHz. The modulation amplitude was 0.05 mT for $HEXA_{1,5}$, 0.10 mT for $HEPTA_{3,6}$, and 0.03 mT for the other peptides. Only one scan was needed per level of power attenuation, except for the peptides $HEXA_{1,5}$ and $HEPTA_{3,6}$, for which up to 36 scans per level of power attenuation were done to increase the signal-to-noise ratio. To monitor the temperature in the dielectric cavity, a chromel/alumel thermocouple with a readability of 0.1 K was used. A constant stream of N_2 was sent through the cavity to maintain a temperature of 293 K.

Theoretical aspects

A saturation curve is obtained in cw mode by measuring the amplitude Y of a first-derivative EPR line (see Figure 4.1) as a function of the microwave power P. The shape of the saturation curve is, amongst others, determined by the product T_1T_2 [7]

$$Y \propto \frac{B_1}{\left(1+B_1^2\gamma^2T_1T_2\right)^{\varepsilon}} \tag{4.1}$$

where B_1 is the microwave magnetic field, $\gamma = g_e\mu_B/\hbar$, and ε is a measure for the homogeneity of the saturation. For a homogeneously broadened (Lorentzian) line, $\varepsilon = 1.5$. For an inhomogeneously broadened (Gaussian) line, $\varepsilon = 0.5$. In order to determine T_1T_2 form the saturation curve, the amplitudes are fitted to[8]

$$Y = \frac{I\sqrt{P}}{\left[1+\left(2^{1/\varepsilon}-1\right)P/P_{½}\right]^{\varepsilon}}, \tag{4.2}$$

where *I* is a scaling factor. The combination of equations 4.1 and 4.2 gives

$$P_{½} = \frac{2^{1/\varepsilon}-1}{\Lambda^2\gamma^2T_1T_2}, \tag{4.3}$$

where Λ is the resonator efficiency[9]

$$\Lambda = \frac{B_1}{\sqrt{P}}. \tag{4.4}$$

4.3 Results

The cw spectra of peptides $OCTA_7$ and $HEPTA_{3,6}$ are shown in Figure 4.1 and are representative for three-line spectra of class II and five-line spectra of class I peptides, respectively. The lines are referred to with $m_i = +1,\ 0,\ -1$ and $M_I = +2,\ +1,\ 0,\ -1,\ -2$. The cw-EPR spectra of all peptides in this study are shown and analysed in reference [4]. For power saturation measurements, the complete spectra were measured at 31 power settings. Care was taken to measure each compound under comparable conditions (see Material and methods). The line intensities were obtained as shown by the red arrows in Figure 4.1 and plotted as a function of $\sqrt{P}$ (Figure 4.2).

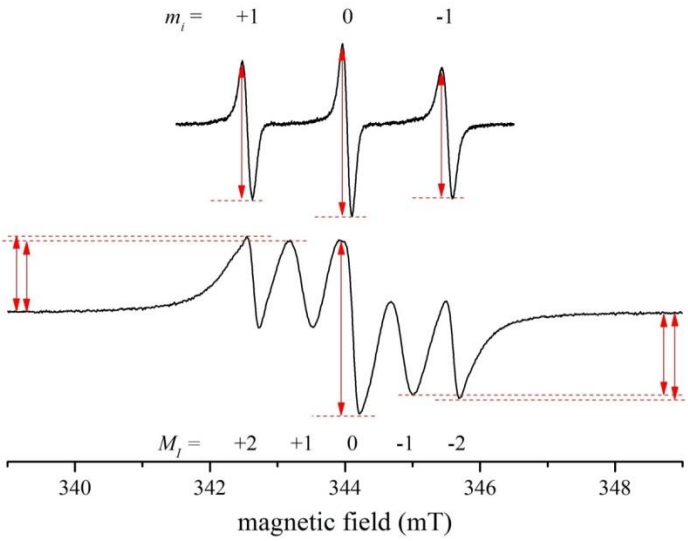

Figure 4.1 Typical cw-EPR spectra of the peptides investigated here. The top spectrum, of $OCTA_7$, is typical for mono-radicals and class II bi-radicals (conditions: one scan at 63.3 mW). The bottom spectrum, of $HEPTA_{3,6}$, is typical for class I bi-radicals (conditions: 25 scans accumulated at 25.2 mW). The indexes $m_i = +1,\ 0,\ -1$ and $M_I = +2,\ +1,\ 0,\ -1,\ -2$ are used to refer to the three and five spectral lines, respectively. The red arrows show how the first-derivative amplitudes of the spectral lines were measured in the respective spectra.

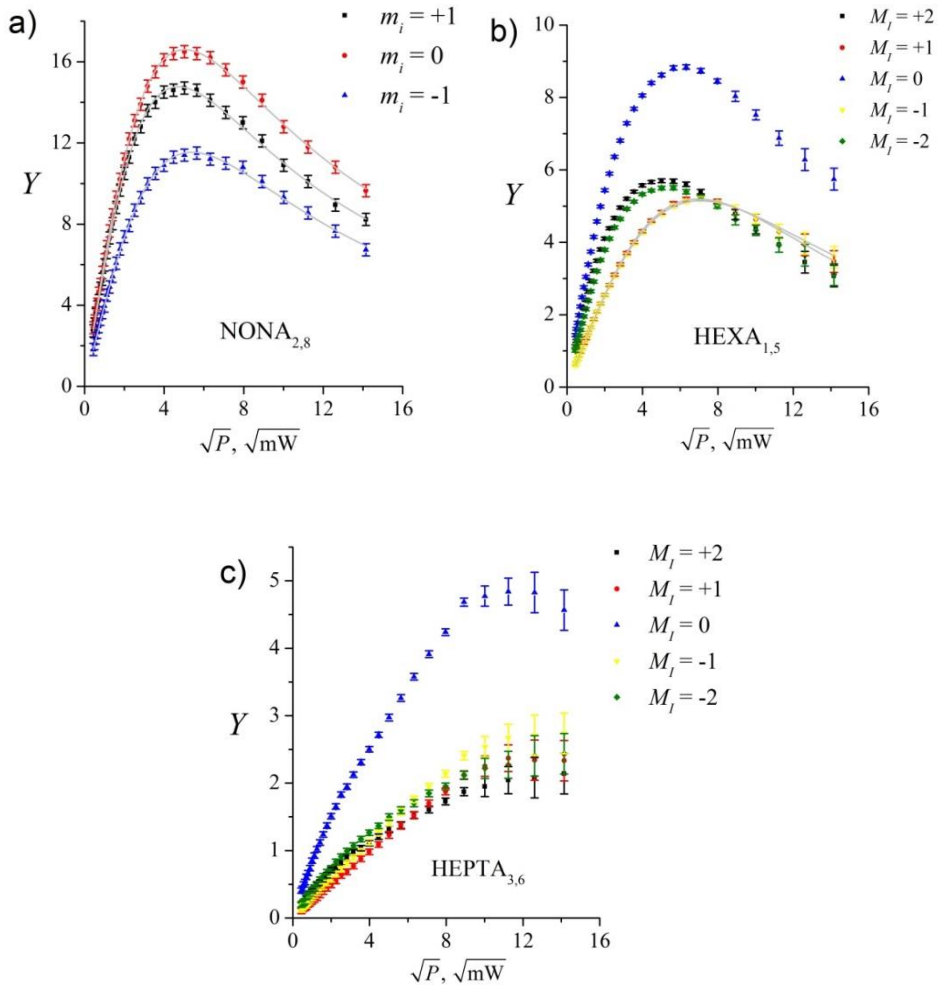

Figure 4.2 Examples of saturation curves for mono-radical and class I peptides ($NONA_{2,8}$) and the two class II peptides ($HEXA_{1,5}$ and $HEPTA_{3,6}$) with the first-derivative amplitudes plotted against $\sqrt{P}$. Note that because of the definition of the amplitude (Figure 4.1), the amplitude of the $M_I = 0$ component is twice that of the remaining components. For each amplitude, the error bar is taken as twice the amplitude of the noise. The saturation curves that could be fitted to equation 4.2 are shown as grey lines.

The fits according to equation 4.2 (shown in Figure 4.2 as grey lines) yield the characteristic powers of half-saturation ($P_{½}$) and parameters ε, which are listed in Table 4.1. The powers $P_{½}$, which we discuss first, reflect the ease of saturation. For peptides $NONA_9$, $NONA_{2,8}$, $HEPTA_6$, $OCTA_{2,7}$, and $OCTA_7$, $P_{½}$ increases in the order of decreasing m_i, similar to the trend in increasing linewidths[4]. In the saturation curves for the $HEXA_{1,5}$ (Figure 4.2b), the $M_I = \pm 2$ and 0 components saturate differently than the $M_I = \pm 1$ components. The initial linear part of the curve is steeper, for $M_I = \pm 2$ and 0, and the maximum of the amplitude is reached at lower powers than for the $M_I = \pm 1$ component. The saturation behaviour of the $M_I = \pm 1$ component is fitted by equation 4.2, yielding the parameters given in Table 4.1. For the $M_I = \pm 2$ and 0 components the curves cannot be fitted with meaningful values. Also, fitting with two components did not yield unique solutions. Therefore, only values for the $M_I = \pm 1$ components can be determined. Also, for this peptide no significant difference is observed between the $P_{½}$ values of the $M_I = \pm 1$ and $M_I = -1$ lines. For peptide $HEPTA_{3,6}$, the maximally available power of the instrument was not sufficient to reach full saturation (Figure 4.2c), therefore only a lower limit for $P_{½}$ can be determined: $P_{½} > 200$ mW.

The ε values, which reflect whether the line is Lorentzian (ε = 1.5) or Gaussian (ε = 0.5), for most compounds are in the range for mixtures of these two fundamental lineshapes, showing that the lines are partially inhomogeneously broadened, presumably on account of hyperfine broadening. Only $HEXA_{1,5}$ has an ε value (ε = 1.5) appropriate for a purely Lorentzian line, showing that the lineshape for this bi-radical is determined by a process,

which is so fast that it dominates the lineshape. For none of the compounds a purely Gaussian saturation behaviour (ε = 0.5) is seen.

Table 4.1 Relaxation parameters of mono- and bi-radical peptides.

		$m_I = +1$		$m_I = 0$		$m_I = -1$	
		$P_{½}$ (mW) [a]	ε [b]	$P_{½}$ (mW) [a]	ε [b]	$P_{½}$ (mW) [a]	ε [b]
$NONA_9$		11.5	1.02	14.4	1.02	18.5	1.18
$NONA_{2,8}$		23.2	1.09	26.9	1.11	31.5	1.18
	$\Delta P_{½}$	11.7	N.A.	12.5	N.A.	13	N.A.
$OCTA_7$		11.3	0.95	13.3	0.94	16.9	1.1
$OCTA_{2,7}$		16.8	0.87	19.8	1.02	24.4	1.05
	$\Delta P_{½}$	5.6	N.A.	6.5	N.A.	7.5	N.A.
$HEPTA_6$		13.1	0.83	16.8	0.84	21.2	1.02
		$M_I = +1$		N.A.		$M_I = -1$	
$HEXA_{1,5}$		58.6	1.5			58.6	1.5
	$\Delta P_{½}$ [c]	45.5	N.A.			37.4	N.A.
$HEPTA_{3,6}$		> 200	N.A.			> 200	N.A.
	$\Delta P_{½}$ [c]	> 200	N.A.			> 200	N.A.

[a] The error in P½ due to fitting is less than 2%.

[b] The error in ε due to fitting is less than 2%, except for HEXA1,5: less than 5%.

[c] with respect to M_I = +1 and M_I = -1 in $HEPTA_6$.

With values for $P_{½}$ and ε, we can in principle use equation 4.3 to calculate the product T_1T_2 of the peptides. However, the resonator efficiency Λ of the dielectric cavity has to be determined first. Finding Λ is presently under study. For now, we shall analyse the data in terms of $\Delta P_{½}$, which is the difference between the $P_{½}$ values of the mono- and bi-radicals:

$$\Delta P_{½} = P_{½\ \text{biradical}} - P_{½\ \text{monoradical}}\ . \tag{4.5}$$

The resulting $\Delta P_{½}$ values are listed in Table 4.1. Notably, for peptides $NONA_{2,8}$, and $OCTA_{2,7}$ the $\Delta P_{½}$ values do not differ significantly with respect to m_i.

4.4 Discussion

Reliable power-saturation curves have been obtained for all species investigated in this study. By excluding oxygen from the samples, Heisenberg exchange by oxygen as an additional relaxation source is avoided.

Saturation behaviour is expressed in the parameters ε and $P_{½}$. We first discuss the ε parameters of all compounds. The ε values agree with the results of the lineshape simulations performed previously, with the exception of $HEXA_{1,5}$. The latter bi-radical saturates as a pure Lorentzian (ε = 1.5), whereas the lineshape was simulated with a mixture of Gaussian and Lorentzian lines. The origin of this discrepancy may be the two-component nature of the cw-EPR spectrum (see below). The fast relaxation in $HEPTA_{3,6}$ prevents the determination of ε.

Equation 4.3 shows that $P_{½}$ is inversely proportional to the product T_1T_2, therefore, large $P_{½}$ values are identified with fast relaxation and, unless specified otherwise, we refer to relaxation as the product of the two relaxation times.

The parameters obtained for $P_{½}$ show systematic trends. For the mono-radicals and the class II bi-radicals, the $P_{½}$ values decrease with increasing m_i, suggesting a spin-spin relaxation process, because, for nitroxides, the spin-spin relaxation time T_2 is m_i dependent[10-13] which is not the case for T_1, see for example[14]. In particular, T_2 increases with increasing m_i, and since T_2 is inversely proportional to $P_{½}$, a decrease in $P_{½}$ with increasing m_i is fully consistent with a T_2 process.

To compare the mono- and bi-radical relaxation we use the difference of $P_{½}$ values ($\Delta P_{½}$, equation 4.5). To avoid interference from different

relaxation mechanisms, $\Delta P_{½}$ values are given for the same m_i – transitions as much as possible.

The two class I bi-radicals $HEPTA_{3,6}$ and $HEXA_{1,5}$ are in the regime of strong exchange interaction[4] and, considering their $P_{½}$ values (Table 4.1), relax significantly faster than their mono-radical reference $HEPTA_6$ and the class II bi-radicals. For $HEPTA_{3,6}$ this relaxation is even so fast that only a lower limit for $P_{½}$ can be given. The saturation of three of the five lines of the $HEXA_{1,5}$ bi-radical (components M_I = ± 2 and 0) could not be fitted to equation 4.2, whereas the M_I = ±1 components could. Previously, the EPR spectra of this bi-radical were shown to consist of two species, one that has a five-line spectrum and one with a three-line spectrum, the three lines of which overlap with the M_I = ± 2 and 0 lines of the five-line spectrum. The two species were speculated to derive from two conformations of the bi-radical, a majority-fraction with a high J value and a minority-fraction of low J [4]. The presence of two species with presumably different relaxation behaviour that contribute to the M_I = ± 2 and 0 components will produce power saturation curves that consist of a superposition of curves with different $P_{½}$ and ε values. We could not find models that consistently describe these curves, presumably due to the large number of parameters that have to be fit. The $\Delta P_{½}$ values given for $HEXA_{1,5}$ derive from the M_I = ±1 components of the bi-radical and the m_i = ±1 of the mono-radical. The M_I = ±1 line connects m_i = 0 and m_i = ±1 transitions, and therefore, the $\Delta P_{½}$ value can contain a contribution, which is m_i dependent.

The $P_{½}$ values of class II bi-radicals, similar to the class I bi-radicals, are larger than their mono-radical references. The $\Delta P_{½}$ values hardly depend on

m_i, an indication that mono- and bi-radical have similar T_2 values. This is expected, because the spin-spin relaxation time T_2 is associated with the rotation-correlation time of the peptides, and mono- and bi-radical peptides are size-matched and therefore should have very similar rotation-correlation times. This also shows that the additional relaxation mechanism operating in the bi-radicals is most likely a T_1-process. So we speculate that the spin-spin interaction in the bi-radicals opens another channel for T_1 relaxation.

In all four bi-radicals an additional relaxation process must be operative, and for the class II bi-radicals we show evidence that it is likely to be a T_1 process. For class I bi-radicals the additional relaxation process is stronger, leading to larger $\Delta P_{½}$ values than in class II bi-radicals. A quantitative comparison for class I bi-radicals is not straightforward. The $\Delta P_{½}$ values of one of these bi-radicals ($HEXA_{1,5}$) contains a contribution from different m_i transitions, and in that case we cannot exclude that also T_2 affects the $\Delta P_{½}$ values. For the second one of the class I bi-radicals, $HEPTA_{3,6}$, only a lower limit for $P_{½}$ and therefore $\Delta P_{½}$ could be given. Qualitatively, the bi-radical with the shortest distance between the nitroxides, $HEPTA_{3,6}$, has the fastest relaxation.

Within the class II bi-radicals, the $\Delta P_{½}$ value is larger for $NONA_{2,8}$ than for $OCTA_{2,7}$, although for the latter peptide the TOAC residues are closer in the sequence. The through-space distance between the nitroxides in $NONA_{2,8}$ (1.26 nm) is shorter than for $OCTA_{2,7}$ (1.46 nm), showing that the mechanism causing the additional relaxation in class II bi-radicals is related to through-space interactions, rather than through-bond interactions.

Spin-spin interaction can enhance relaxation via the dipole-dipole interaction or via the exchange interaction J. The dipole-dipole interaction

depends only on the distance between the spins, whereas J, generally thought to depend exponentially on distance, also can have a substantial through-bond component. The difference in relaxation of $NONA_{2,8}$ and $OCTA_{2,7}$ cannot be due to a through-bond exchange mechanism, because that would cause faster relaxation in $OCTA_{2,7}$ opposite to what we observe. Also a through-space J interaction mediated process is not likely, because the distances between the spins in both bi-radicals seem too long given the exponential decay of J with distance. Therefore, the dipolar interaction is the most likely candidate. To properly assess this point detailed quantum-mechanical calculations are needed, which we are starting off.

In summary, the important finding is that by power saturation we can discriminate between two bi-radicals, $NONA_{2,8}$ and $OCTA_{2,7}$. These peptides have distances between the spin labels (1.26 nm and 1.46 nm, respectively) in a region that is difficult to address, and have almost identical cw-EPR spectra.

4.5 Conclusions

We show that meaningful power-saturation curves can be obtained at room temperature and at concentrations relevant for biological samples. The signal-to-noise ratio is sufficient to extract the relaxation parameters. We show that two bi-radical peptides, whose cw-EPR spectra are almost identical to those of their related mono-radicals, can be distinguished by their relaxation behaviour, showing that relaxation could be a monitor for distances of about 1.3 and 1.5 nm, right in the range that is difficult to assess for EPR distance determination.

References

[1] A.D. Milov, A.G. Maryasov, Y.D. Tsvetkov, Pulsed electron double resonance (PELDOR) and its applications in free-radicals research. Applied Magnetic Resonance **15** (1998) 107-143.

[2] G. Jeschke, Distance measurements in the nanometer range by pulse EPR. Chemphyschem **3** (2002) 927-932.

[3] J.E. Banham, C.M. Baker, S. Ceola, I.J. Day, G.H. Grant, E.J.J. Groenen, C.T. Rodgers, G. Jeschke, C.R. Timmel, Distance measurements in the borderline region of applicability of CW EPR and DEER: A model study on a homologous series of spin-labelled peptides. Journal of Magnetic Resonance **191** (2008) 202-218.

[4] M.H. Shabestari, M. van Son, A. Moretto, M. Crisma, C. Toniolo, M. Huber, Conformation and EPR Characterization of Rigid, 3(10)-Helical Peptides with TOAC Spin Labels: Models for Short Distances. Biopolymers **102** (2014) 244-251.

[5] S. Carlotto, M. Zerbetto, M.H. Shabestari, A. Moretto, F. Formaggio, M. Crisma, C. Toniolo, M. Huber, A. Polimeno, In Silico Interpretation of cw-ESR at 9 and 95 GHz of Mono- and bis- TOAC-Labeled Aib-Homopeptides in Fluid and Frozen Acetonitrile. Journal of Physical Chemistry B **115** (2011) 13026-13036.

[6] M. Zerbetto, S. Carlotto, A. Polimeno, C. Corvaja, L. Franco, C. Toniolo, F. Formaggio, V. Barone, P. Cimino, Ab initio modeling of CW-ESR spectra of the double spin labeled peptide Fmoc-(Aib-Aib-TOAC)(2)-Aib-OMe in acetonitrile. Journal of Physical Chemistry B **111** (2007) 2668-2674.

[7] C.P. Poole, Electron Spin Resonance, Wiley, New York, 1983.

[8] C. Altenbach, W. Froncisz, R. Hemker, H. Mchaourab, W.L. Hubbell, Accessibility of nitroxide side chains: Absolute Heisenberg exchange rates from power saturation EPR. Biophysical Journal **89** (2005) 2103-2112.

[9] W. Froncisz, J.S. Hyde, The Loop-Gap Resonator - A New Microwave Lumped Circuit Electron-Spin-Resonance Sample Structure. Journal of Magnetic Resonance **47** (1982) 515-521.

[10] P.W. Atkins, D. Kivelson, ESR Linewidths in Solution .2. Analysis of Spin-Rotational Relaxation Data. Journal of Chemical Physics **44** (1966) 169-174.

[11] D.E. Budil, S. Lee, S. Saxena, J.H. Freed, Nonlinear-least-squares analysis of slow-motion EPR spectra in one and two dimensions using a modified Levenberg-Marquardt algorithm. Journal of Magnetic Resonance Series A **120** (1996) 155-189.

[12] R. Cassol, A. Ferrarini, P.L. Nordio, Dynamics of Nitroxide Probes Linked to Flexible Chains. Journal of Physical Chemistry **97** (1993) 2933-2940.

[13] G. Moro, P.L. Nordio, U. Segre, Electron-Spin-Resonance Lineshapes of Free-Radicals Undergoing Jump Diffusion. Gazzetta Chimica Italiana **109** (1979) 585-588.

[14] C. Galli, J.B. Innes, D.J. Hirsh, G.W. Brudvig, Effects of dipole-dipole interactions on microwave progressive power saturation of radicals in proteins. Journal of Magnetic Resonance Series B **110** (1996) 284-287.